

Search for radiative B meson decays

The Crystal Ball Collaboration

T. Lesiak⁴, D. Antreasyan⁹, H.W. Bartels⁵, D. Besset¹¹, Ch. Bieler⁸, J.K. Bienlein⁵,
A. Bizzeti⁷, E.D. Bloom¹², I. Brock³, K. Brockmüller⁵, R. Cabenda¹¹, A. Cartacci⁷,
M. Cavalli-Sforza², R. Clare¹², A. Compagnucci⁷, G. Conforto⁷, S. Cooper^{12,a}, R. Cowan¹¹,
D. Coyne², A. Engler³, K. Fairfield¹², G. Folger⁶, A. Fridman^{12,b}, J. Gaiser¹²,
D. Gelphman¹², G. Glaser⁶, G. Godfrey¹², K. Graaf⁸, F.H. Heimlich⁷, F.H. Heinsius⁸,
R. Hofstadter^{12,c}, J. Irion⁹, Z. Jakubowski⁵, H. Janssen¹⁰, K. Karch⁵, S. Keh¹³, T. Kiel⁸,
H. Kilian¹³, I. Kirkbride¹², T. Kloiber⁵, M. Kobel⁶, W. Koch⁵, A.C. König¹⁰,
K. Königsmann^{13,d}, R.W. Kraemer³, S. Krüger⁸, G. Landi⁷, R. Lee¹², S. Leffler¹²,
R. Lekebusch⁸, A.M. Litke¹², W. Lockman¹², S. Lowe¹², B. Lurz⁶, D. Marlow³,
H. Marsiske^{5,12}, W. Maschmann⁵, P. McBride⁹, F. Messing³, W.J. Metzger¹⁰, H. Meyer⁵,
B. Monteleoni⁷, B. Muryn^{4,e}, R. Nernst⁸, B. Niczyporuk¹², G. Nowak⁴, C. Peck¹,
P.G. Pelfer⁷, B. Pollock¹², F.C. Porter¹, D. Prindle³, P. Ratoff¹, M. Reidenbach¹⁰,
B. Renger³, C. Rippich³, M. Scheer¹³, P. Schmitt¹³, J. Schotanus¹⁰, J. Schütte⁶,
A. Schwarz¹², D. Sievers⁸, T. Skwarnicki⁵, V. Stock⁸, K. Strauch⁹, U. Strohmusch⁸,
J. Tompkins¹², H.J. Trost⁵, B. van Uitert¹², R.T. Van de Walle¹⁰, H. Vogel³, A. Voigt⁵,
U. Volland⁶, K. Wachs⁵, K. Wacker¹², W. Walk¹⁰, H. Wegener⁶, D. A. Williams^{9,2},
P. Zschorsch⁵

¹ California Institute of Technology^f, Pasadena, CA 91125, USA

² University of California at Santa Cruz^g, Santa Cruz, CA 95064, USA

³ Carnegie-Mellon University^h, Pittsburgh, PA 15213, USA

⁴ Cracow Institute of Nuclear Physics, PL-30055 Cracow, Poland

⁵ Deutsches Elektronen Synchrotron DESY, D-2000 Hamburg, Germany

⁶ Universität Erlangen-Nürnbergⁱ, D-8520 Erlangen, Germany

⁷ INFN and University of Firenze, I-50125 Firenze, Italy

⁸ Universität Hamburg, I. Institut für Experimentalphysik^k, D-2000 Hamburg, Germany

⁹ Harvard University^l, Cambridge, MA 02138, USA

¹⁰ University of Nijmegen and NIKHEF^m, NL-6525 ED Nijmegen, The Netherlands

¹¹ Princeton Universityⁿ, Princeton, NJ 08544, USA

¹² Department of Physics^o, HEPL, and Stanford Linear Accelerator Center^p,
Stanford University, Stanford, CA 94309, USA

¹³ Universität Würzburg^r, D-8700 Würzburg, Germany

Abstract

The Crystal Ball detector at the e^+e^- storage ring DORIS-II has been used to search for radiative B meson decays, especially of the type $b \rightarrow s\gamma$. No mono-energetic γ -lines have been found in the inclusive photon spectrum from $\Upsilon(4S)$ decays, and upper limits are obtained for radiative decays of B mesons to various strange mesons and to the D^* . Integrating the photon spectrum over the corresponding energy range, we find

$$BR(B \rightarrow \gamma X) < 2.8 \times 10^{-3}$$

at 90% confidence level for the mass range $892 \text{ MeV} \leq M_X \leq 2045 \text{ MeV}$.

-
- a) Present address: Max-Planck-Institut für Physik, D-8000 München 40, Germany
 - b) Permanent address: DPHPE, Centre d'Etudes Nucléaires de Saclay, F-91191 Gif sur Yvette, France
 - c) deceased
 - d) Present address: CERN, CH-1211 Genève 23, Switzerland
 - e) Permanent address: Institute of Physics and Nuclear Techniques, AGH, PL-30055 Cracow, Poland
 - f) Supported by the U.S. Department of Energy, contract No. DE-AC03-81ER40050 and by the National Science Foundation, grant No. PHY75-22980
 - g) Supported by the National Science Foundation, grant No. PHY85-12145
 - h) Supported by the U.S. Department of Energy, contract No. DE-AC02-76ER03066
 - i) Supported by the German Bundesministerium für Forschung und Technologie, contract No. 054 ER 12P(5)
 - k) Supported by the German Bundesministerium für Forschung und Technologie, contract No. 054 HH 11P(7) and by the Deutsche Forschungsgemeinschaft
 - l) Supported by the U.S. Department of Energy, contract No. DE-AC02-76ER03064
 - m) Supported by FOM-NWO
 - n) Supported by the U.S. Department of Energy, contract No. DE-AC02-76ER03072 and by the National Science Foundation, grant No. PHY82-08761
 - o) Supported by the U.S. Department of Energy, contract No. DE-AC03-76SF00326 and by the National Science Foundation, grant No. PHY81-07396
 - p) Supported by the U.S. Department of Energy, contract No. DE-AC03-76SF00515
 - r) Supported by the German Bundesministerium für Forschung und Technologie, contract No. 054 WU 11P(1)

1 Introduction

The existence of flavour changing neutral currents between b and s quarks, leading to radiative transitions $b \rightarrow s\gamma$, is predicted by the Standard Model [1] and by its extensions such as left-right symmetric theories [2], models with a fourth fermion generation [3] or two Higgs doublets [4], and supersymmetric models [5]. As shown in Fig. 1, $b \rightarrow s\gamma$ may occur in the Standard Model through one-loop penguin diagrams [6]. The branching ratio depends on the top quark mass m_t , and is increased by an order of magnitude by QCD radiative corrections [7,8]. A recent calculation gives $BR(b \rightarrow s\gamma) = 4.4 \times 10^{-4}$ for $m_t = 120 \text{ GeV}$ and $\Lambda_{QCD} = 200 \text{ MeV}$ [9]. It is believed that the final states are dominated by K^* mesons, but the predictions for the branching ratios vary widely; for example, estimates for $\Gamma(B \rightarrow K^*(892)\gamma)/\Gamma(b \rightarrow s\gamma)$ range from 4.5% to 40% [8,10].

In this paper we use the inclusive photon spectrum from B meson decays to search for the process $b \rightarrow s\gamma$ [11]. We derive upper limits for two-body exclusive decays $B \rightarrow K^*\gamma$, where K^* denotes different kaon spin-parity states. We concentrate on four of them, namely $K^*(892)$, $K_1(1400)$, $K_2(1770)$ and $K_4^*(2045)$, which should be representative of other K^* 's with similar masses. To avoid depending on the theoretical branching ratios to the individual K^* 's, we also derive an inclusive limit for the decay $b \rightarrow s\gamma$ [12] by integrating the photon spectrum over the relevant energy range.

2 Detector

The Crystal Ball detector (described in detail in [13] and [14]) is designed to measure precisely the energy and direction of electromagnetically showering particles. The energy resolution is $\sigma_E/E = (2.7 \pm 0.2)\%/\sqrt{E/\text{GeV}}$ and the polar angle resolution varies between 1° and 3° , depending on the photon energy. The major part of the detector – a non-magnetic calorimeter – is a spherical shell of 672 NaI(Tl) crystals covering 93% of $4\pi\text{sr}$ solid angle. The thickness of the shell corresponds to 16 radiation lengths or one nuclear interaction length. Each crystal has the shape of a truncated triangular pyramid pointing to the e^+e^- interaction point. Charged particles are detected in four double layers of proportional tube chambers placed inside the ball surrounding the beam pipe cylindrically. The outermost layer covers 78% of $4\pi\text{sr}$.

All events used in this study satisfy our total energy trigger, that is, they deposit at least 1.9 GeV in the NaI(Tl) crystals of the main calorimeter excluding the 60 crystals surrounding the beam pipe (covering 83% of $4\pi\text{sr}$ solid angle).

3 Event selection

The data used in this analysis were taken at the DORIS-II e^+e^- storage ring on the $\Upsilon(4S)$ resonance (ON $\Upsilon(4S)$ data) at a beam energy of $(5.290 \pm 0.005) \text{ GeV}$ and in the continuum below this resonance in the beam energy range from 5.230 GeV to 5.260 GeV . The integrated luminosity of these two data samples is 75.9 pb^{-1} and 18.5 pb^{-1} , respectively.

3.1 Selection of hadronic events

We first select multi-hadron events using the criteria described in [14]. We find that the number of multi-hadronic events is $N_{ON}^{had} = 288.6 \times 10^3$ in the ON $\Upsilon(4S)$ and $N_{cont}^{had} = 56.7 \times 10^3$ in the continuum data. The number of observed hadronic events arising from the $\Upsilon(4S)$ resonance is then

$$N_{\Upsilon(4S)}^{obs} = N_{ON}^{had} - N_{cont}^{had} \times r = (60.3 \pm 1.1) \times 10^3, \quad (1)$$

where $r = 4.025 \pm 0.009$, the continuum normalization ratio, is the ratio of the numbers of Bhabha events in the ON $\Upsilon(4S)$ and in the continuum data sample. The error of 1.7% on $N_{\Upsilon(4S)}^{obs}$ is dominated by the 0.4% statistical error of the continuum sample multiplied by the factor r . Other contributions are a 0.2% statistical uncertainty in r and less than 0.2% from a possible difference of the beam-gas background in the ON $\Upsilon(4S)$ and the continuum data.

3.2 Selection of $B \rightarrow \gamma X$ events

To enhance the ratio of $\Upsilon(4S) \rightarrow B\bar{B}$ events to hadronic continuum events and to further reduce the background from $\tau^+\tau^-$ events, we apply two cuts. We select high multiplicity events by requiring that the energy deposition in the main calorimeter has more than 7 local maxima (which mark particles in the apparatus). Since hadronic events from $\Upsilon(4S)$ decays are more spherical than those from continuum production, we select spherically-symmetric events with the requirement $H_2 < 0.40$. H_2 is the second Fox-Wolfram moment [15] describing the energy-weighted angular topology of an event; it is close to one for jet-like events and is almost zero for spherical events.

We search for photon candidates with energy greater than 1 GeV. To have a reliable charge determination, we use only particles that pass through all four layers of tube chambers by demanding $|\cos\theta| < 0.75$, where θ is the angle between the beam axis and the particle direction. The photon candidate is allowed to have at most one hit in the chambers, which is consistent with the photon direction. The lateral pattern of the energy deposition of photon candidates in the main calorimeter must agree with that expected for electromagnetically showering particles.

The inclusive photon spectrum obtained after these cuts is plotted for ON $\Upsilon(4S)$ and the continuum data in Fig. 2. The energy scale here is logarithmic with a bin size of 3%, which corresponds approximately to the Crystal Ball energy resolution. In Fig. 3 we present the inclusive photon spectrum from $B\bar{B}$ events, i.e., after subtraction of the normalized continuum. No monoenergetic line is seen. As a check of the continuum subtraction, we calculate the total number of photons in the inclusive spectrum from $B\bar{B}$ events in the energy range above 2.7 GeV (see Fig. 3), that is, above the kinematical limit for photons from B meson decay. This results in (8 ± 54) photons.

4 Efficiency calculation

The efficiency for the selection of multi-hadron events is estimated by simulating $\Upsilon(4S)$ decays according to the reaction

$$e^+e^- \rightarrow \Upsilon(4S) \rightarrow B\bar{B} \rightarrow \text{hadrons} \quad (2)$$

using the LUND 6.1 string fragmentation program [16] and passing the generated events through a complete detector simulation. Electromagnetically interacting particles are handled by the program EGS 3 [17]. The interactions of hadrons are simulated with the improved GHEISHA 6 program [18]. Extra energy deposited in the crystals by beam-related background is taken into account by overlying special events, which have been collected by triggering on every 10⁷th beam crossing with no other condition. The Monte Carlo events are then reconstructed with our standard software and subjected to the same cuts as the data. The efficiency of our hadronic selection for $B\bar{B}$ events is found to be

$$\epsilon_{had} = (92.0 \pm 0.5 \pm 0.9)\%. \quad (3)$$

To determine the overall efficiency for selecting $K^*\gamma$ events, we simulate $\Upsilon(4S)$ decays to the $B\bar{B}$ pair where one B meson decays into a photon and a K^* and the other B meson is allowed to decay into the standard channels by the LUND program. The $K^*(892)$ decay is generated with the correct angular distribution, while those for the higher mass K^* 's are approximated by phase space. The efficiency is given as the ratio of the number of selected photons from $K^*\gamma$ events to the number of generated events. This yields:

$$\begin{aligned} \epsilon_{\gamma}^{K^*(892)} &= (13.5 \pm 0.4 \pm 0.8)\% \\ \epsilon_{\gamma}^{K_1(1400)} &= (17.0 \pm 0.6 \pm 0.8)\% \\ \epsilon_{\gamma}^{K_2(1770)} &= (20.4 \pm 0.6 \pm 0.8)\% \\ \epsilon_{\gamma}^{K_1^*(2045)} &= (20.3 \pm 0.6 \pm 0.8)\%, \end{aligned} \quad (4)$$

where the first error is statistical and the second systematic. The latter includes the systematic uncertainty in the choice of the fragmentation function applied in the simulation of the decay of the other B meson (as a measure of this uncertainty we take the difference in efficiencies for the string and Feynman-Field fragmentation functions). For the mode $B \rightarrow K^*(892)\gamma$ we also study the difference in the efficiencies for neutral and charged B meson decays by Monte Carlo. It is found to be 0.3%. The rise of the efficiency for higher mass K^* states is mainly due to the cut on the second Fox-Wolfram moment H_2 . For higher masses of the K^* state, the topology of the event is more symmetrical (smaller values of H_2) as the K^* decays then on average into more particles and at the same time the photon energy becomes smaller.

We performed also Monte Carlo study of the π^0 background from the decays $B \rightarrow D(\text{or } D^*)\rho^+$, $\rho^+ \rightarrow \pi^+\pi^0$ and $B \rightarrow D^*\pi^0(n\pi^\pm)$, where $n = 1, 2, 3$. For the modes $B \rightarrow D\rho^+$, $\rho^+ \rightarrow \pi^+\pi^0$ and $B \rightarrow D^*\rho^+$, $\rho^+ \rightarrow \pi^+\pi^0$ the generated π 's had a $\cos^2 \vartheta$ ($\sin^2 \vartheta$, respectively) angular distribution, where ϑ is the angle between the ρ^+ direction of flight and one of the π 's measured in the ρ^+ rest frame. The decays $B \rightarrow D^*\pi^0(n\pi^\pm)$ have been uniformly generated in phase space. Using the branching ratios for those modes from Ref. [19] we found the number of π^0 's with energy bigger than 2050 MeV (see section. 5) and surviving all cuts to be of 4.1. This confirms that our selection was efficient in reducing the π^0 background.

5 Results

To search for the decays $B \rightarrow K^*\gamma$, we investigate two distributions: the inclusive photon spectrum and the angular distribution between the photon and the 'opposite' particle, i.e.,

the particle with the largest opening angle α with respect to the photon. Because the B meson from $\Upsilon(4S)$ decay has a very low momentum ($\cong 320 \text{ MeV}/c$), the photon and the K^* must have almost opposite directions. This should manifest itself in the presence of at least one particle at an angle to the selected photon close to 180° . For each of the distributions in question, we calculate the likelihood simultaneously for ON $\Upsilon(4S)$ and continuum data assuming Poissonian error distribution.

In fits to the inclusive photon spectra of Fig. 2, the signal shape, as determined from the Monte Carlo, is parametrized by the function

$$f(x) = \frac{C}{1 + \exp\left(\frac{|x - \bar{x}| - \sigma_x/2}{z}\right)}, \quad (5)$$

where C normalizes the function to unit area, x is the logarithm of the photon energy, σ_x describes the Doppler broadening of the photon line from the decay $B \rightarrow K^*\gamma$, and z is the detector's photon energy resolution. The background is parameterized by the function $a + bx$, which gives a good fit to the continuum data. The ON $\Upsilon(4S)$ data are parametrized by $N_\gamma f + R(a + bx)$, where the fit parameters N_γ and R correspond to the number of photons and the continuum normalization ratio, respectively. The likelihood function is

$$\begin{aligned} \mathcal{L} &= \mathcal{L}_{ON}(Y, N) \times \mathcal{L}_{CONT}(V, M) \times \mathcal{L}_{lum} \\ &= \left(\prod_i \frac{Y_i^{N_i} \cdot \exp(-Y_i)}{N_i!} \right) \times \left(\prod_k \frac{V_k^{M_k} \cdot \exp(-V_k)}{M_k!} \right) \times \left(\exp\left(-\frac{(R - r)^2}{2\sigma_r^2}\right) \right), \end{aligned} \quad (6)$$

where N_i and M_i are the numbers of selected photons in the i^{th} bin of the ON $\Upsilon(4S)$ and the continuum spectra while the respective numbers resulting from the fit are Y_k and V_k . Here the first and second factors represent the likelihoods for the ON $\Upsilon(4S)$ data and the continuum data. The number of fitted background events in the ON $\Upsilon(4S)$ spectrum is constrained by the third factor in the likelihood function to be nearly equal to the fitted continuum contribution multiplied by the continuum normalization ratio factor. The strength of this constraint is given by the parameter $\sigma_r = 0.009$, the error on r . The fit results give R within one sigma of r .

For each K^* , the $\cos \alpha$ distribution of the photons in the corresponding energy range for ON $\Upsilon(4S)$ data and continuum data, is plotted. The ON $\Upsilon(4S)$ distribution for the $K^*(2045)$ case is shown in Fig. 4. The corresponding distribution from a Monte Carlo simulation of $B \rightarrow K^*(2045)\gamma$, also shown in Fig. 4, is more sharply peaked towards $\cos \alpha = -1$ than the data. The difference is more pronounced for the lower mass K^* states. This shows that the angular distribution can add to our discrimination between $K^*\gamma$ decays and other B decays or continuum events. To exploit this, we make joint fits to the photon spectrum and the $\cos \alpha$ distribution for each K^* state. The angular distribution expected for a $B \rightarrow K^*\gamma$ signal is parametrized by a Gaussian with the mean at $\cos \alpha = -1$ and with the width obtained from the fits to the respective Monte Carlo distributions. The background is parametrized by a constant plus a quadratic term ($c + d \cos^2 \alpha$). The likelihood function given in Eq. 6 is multiplied by corresponding factors for the ON $\Upsilon(4S)$ and continuum angular distributions. As an example, we present in Fig. 5 the joint fit for the mode $B \rightarrow K^*(892)\gamma$.

Because the fits for different K^* spin states do not give statistically significant signal amplitudes above background (see Table 1), we convert them to 90% C.L. upper limits on

the branching ratios by numerically integrating the likelihood function for the branching ratio

$$BR = \frac{N_\gamma/\epsilon_\gamma^{K^*}}{2N_{\Upsilon(4S)}^{obs}/\epsilon_{had}},$$

taking into account the errors in the efficiencies and in the number of $B\bar{B}$ pairs [20]. The resulting limits from fits with and without the angular distributions are listed in Table 1. We also present there limits on $B \rightarrow D^*(2010)\gamma$, using the same efficiency as for the $K_4^*(2045)$. For each of the K^* 's and for the D^* , use of the angular distribution improves the limit, as expected. However, except for the $K^*(892)$, the K^* 's decay isotropically in our Monte Carlo, which should be a reasonable approximation for these multi-body decays. A deviation from isotropy should have little effect on the photon spectrum, but its effect on limits obtained using the angular distribution is hard to quantify. Therefore, for conservative upper limits we must rely on the photon distribution alone for the heavier K^* 's.

From the photon spectrum, we also derive an upper limit on the branching ratio for the process $B \rightarrow \gamma X$, where by X we denote any hadron state in the mass range between the $K^*(892)$ and the $K_4^*(2045)$ taking into account the Doppler shift and the energy resolution of the detector. The corresponding photon energies range from 2700 MeV to 2050 MeV. In this energy range the total number of photons is (-61 ± 58) . Assuming that our efficiency in the range in question is the mean value of efficiencies from Eq. 5 we find a 90% C.L. upper limit on the branching ratio for the decay $B \rightarrow \gamma X$ of $BR(B \rightarrow \gamma X) < 2.8 \times 10^{-3}$. If we extend the mass range up to 2800 MeV and assume the same value of the efficiency, we find 3.7×10^{-3} . Assuming that all strange states are in the given mass range and that s quarks fragment with 100% probability to X_s , our limit is valid also for the $b \rightarrow s\gamma$ transition.

Alternatively, a limit on $b \rightarrow s\gamma$ can be derived from our limit on $B \rightarrow K^*(892)\gamma$ and theoretical calculations of the ratio $\Gamma(B \rightarrow K^*(892)\gamma)/\Gamma(b \rightarrow s\gamma)$. Calculations for that ratio range from 4.5% [8] to 40% [10]. Using 4.5% we obtain $BR(b \rightarrow s\gamma) < 3.3 \times 10^{-2}$; for 40% our limit is $< 3.7 \times 10^{-3}$. We see from these values that the method of the previous paragraph, obtaining the $b \rightarrow s\gamma$ limit directly from the photon spectrum, is more powerful in our experiment. It also has the advantage of being relatively model-independent.

6 Conclusions

We have not seen any monoenergetic photon line in the inclusive spectrum of high-energy photons coming from $\Upsilon(4S)$ decays. In particular, we obtain the 90% C.L. upper limits

$$\begin{aligned} BR(B \rightarrow K^*(892)\gamma) &< 1.5 \times 10^{-3} \\ BR(B \rightarrow K_1(1400)\gamma) &< 1.6 \times 10^{-3} \\ BR(B \rightarrow K_2(1770)\gamma) &< 1.2 \times 10^{-3} \\ BR(B \rightarrow K_4^*(2045)\gamma) &< 1.0 \times 10^{-3} \\ BR(B \rightarrow D^*(2010)\gamma) &< 1.1 \times 10^{-3}. \end{aligned}$$

For the heavier K^* 's, these limits are stronger than recent CLEO [21] and ARGUS [22] results (see Table 2). We do not give explicit estimates for other K^* states. However, due to the small difference in the photon energies, the limits on the $K^*(1715)$ and $K_3^*(1780)$ must be

similar to the one we quote for the $K_2(1770)$. The same is valid for the $K_1(1400)$, $K^*(1415)$, $K_0^*(1430)$ and $K_2^*(1430)$.

We also look inclusively for $b \rightarrow s\gamma$ by integrating the photon spectrum over the range corresponding to $892 \text{ MeV} \leq M(X) \leq 2045 \text{ MeV}$. Assuming 100% fragmentation of the s quarks to states within this range, we obtain

$$BR(b \rightarrow s\gamma) < 2.8 \times 10^{-3}.$$

This limit is of the same level as recent CLEO and ARGUS results (see Table 3), but free from theoretical assumptions e.g., on the ratio $\Gamma(B \rightarrow K^*(892)\gamma)/\Gamma(b \rightarrow s\gamma)$. Thus it provides an alternative confirmation of the results of other experiments. However, it is still an order of magnitude higher than the recent predictions [9].

Acknowledgements

We would like to thank the DESY and SLAC directorates for their support. This experiment would not have been possible without the dedication of the DORIS machine group as well as the experimental support groups at DESY. Those of us from abroad wish to thank the DESY laboratory for the hospitality extended to us while working at DESY.

Z.J., T.L., B.Muryn, and G.N. thank DESY for financial support. D.W. acknowledges support from the National Science Foundation. E.D.B., R.H., and K.S. have benefitted from financial support from the Humboldt Foundation. K.Königsmann acknowledges support from the Heisenberg Foundation.

References

- [1] M.A. Shifman, in *Proceedings of the International Symposium on Lepton and Photon Interactions at High Energies*, W. Bartel and R. Rückl, Eds. (North Holland, Amsterdam, 1988);
J. Ellis and P.J. Franzini, in *Proceedings of the Workshop on a Heavy Quarks Factory and Nuclear Physics Facility with Superconducting Linacs*, Courmayeur Workshop (1987) 341
- [2] D. Cocolicchio, G. Costa, G.L. Fogli, A. Masiero, Phys. Rev. **D 40** (1989) 1477
- [3] W.S. Hou, A. Soni, H. Steger, Phys. Lett. **B192** (1987) 441;
J.H. Hewett, Phys. Lett. **B193** (1987) 327
- [4] W.S. Hou, R.S. Willey, Phys. Lett. **B202** (1988) 591;
B. Grinstein and M. Wise, Phys. Lett. **B201** (1988) 274
- [5] S. Bertolini, F. Borzumati, A. Masiero, Phys. Lett. **B192** (1987) 437
- [6] T. Inami, C.S. Lim, Progr. Theor. Phys. **65** (1981) 297;
N.G. Deshpande, G. Eilam, Phys. Rev. **D 26** (1982) 2463
- [7] S. Bertolini, F. Borzumati, A. Masiero, Phys. Rev. Lett. **59** (1987) 180;
B. Grinstein, R. Springer, M.B. Wise, Phys. Lett. **B202** (1988) 138; Nucl. Phys. **B339** (1990) 269;
R. Grigjanis, P.O'Donnell, M. Sutherland and H. Navelet, Phys. Lett. **B213** (1989) 355; **B224** (1989) 209
- [8] N.G. Deshpande et al., Phys. Rev. Lett. **59** (1987) 183
- [9] G. Cella et al., Phys. Lett. **B 248** (1990) 181
- [10] T. Altomari, Phys. Rev. **D 37** (1988) 677
- [11] T. Lesiak, Ph.D. Thesis, Cracow Institute of Nuclear Physics, in preparation
- [12] A. Ali, C. Greub, Z. Phys. **C49** (1991) 431; Phys. Lett. **B259** (1991) 182
- [13] E.D. Bloom and C.W. Peck, Ann. Rev. Nucl. Part. Sci. **33** (1983) 143
- [14] K. Wachs et al., Z. Phys. **C42** (1989) 33
- [15] G.C. Fox, S. Wolfram, Phys. Rev. Lett. **41** (1978) 1581
- [16] T. Sjöstrand, CERN Pool Program W5035 (1985); Comp. Phys. Comm. **39** (1986) 347
- [17] R. Ford and W. Nelson, preprint SLAC-210 (1978), unpublished
- [18] H. Fesefeldt, PITHA 85/02, unpublished;
Z. Jakubowski, M. Kobel, Nucl. Instr. Meth. **A297** (1990) 60
- [19] H. Albrecht et al., Z. Phys. **C48**, (1990) 543
- [20] F. James in *Proceedings of the CERN School of Computing*, Vraona-Attiki, Greece; report CERN-81-03
- [21] P. Avery et al., Phys. Lett. **B223**, (1988) 470
- [22] H. Albrecht et al., Phys. Lett. **B229**, (1989) 304

Table 1: 90% C.L. upper limits on branching ratios for the decays $B \rightarrow K^*\gamma$ and $B \rightarrow D^*(2010)\gamma$. Note that due to the proximity in photon energy of all K^{**} 's the numbers of photons determined by the fits are correlated.

Decay mode	Number of photons N_γ		$BR^{UL} \times 10^4$ (90% C.L.)		$\frac{\chi^2}{NDF}$
	γ spectrum (events)	joint fit (events)	γ spectrum	joint fit	γ spectrum
$B \rightarrow K^*(892)\gamma$	19.7 ± 19.8	8.5 ± 12.5	26.2	14.8	60.0/56 = 1.07
$B \rightarrow K_1(1400)\gamma$	4.6 ± 20.2	-3.0 ± 15.6	16.2	10.6	61.0/56 = 1.09
$B \rightarrow K_2(1770)\gamma$	-0.1 ± 20.3	-10.2 ± 15.8	12.2	7.6	61.1/56 = 1.09
$B \rightarrow K_4^*(2045)\gamma$	-9.5 ± 19.9	-19.2 ± 16.4	10.0	6.6	60.8/56 = 1.09
$B \rightarrow D^*(2010)\gamma$	-6.9 ± 19.9	-17.3 ± 16.1	10.6	6.6	61.0/56 = 1.09

Table 2: Summary of experimental results for $B \rightarrow K^*\gamma$ decays ($BR \times 10^4$ at 90% C.L.). The CLEO and ARGUS results are taken from [21] and [22]. In the present experiment the charged and neutral B meson decays are not distinguished. Therefore only values averaged over decays of charged and neutral B mesons are presented.

Mode	CLEO	ARGUS	Crystal Ball
$B^0 \rightarrow K^{*0}(892)\gamma$	2.8	4.2	14.8
$B^+ \rightarrow K^{*+}(892)\gamma$	5.5	5.2	
$B^0 \rightarrow K_1^0(1270)\gamma$		78.0	16.2
$B^+ \rightarrow K_1^+(1270)\gamma$		66.0	
$B^0 \rightarrow K_1^0(1400)\gamma$		48.0	
$B^+ \rightarrow K_1^+(1400)\gamma$		20.0	
$B^0 \rightarrow K_2^{*0}(1430)\gamma$		4.4	
$B^+ \rightarrow K_2^{*+}(1430)\gamma$		13.0	
$B^0 \rightarrow K^{*0}(1715)\gamma$		22.0	12.2
$B^+ \rightarrow K^{*+}(1715)\gamma$		17.0	
$B^0 \rightarrow K_2^0(1770)\gamma$			
$B^+ \rightarrow K_2^+(1770)\gamma$			
$B^0 \rightarrow K_3^{*0}(1780)\gamma$		110.0	10.0
$B^+ \rightarrow K_3^{*+}(1780)\gamma$		50.0	
$B^0 \rightarrow K_4^{*0}(2045)\gamma$		48.0	10.0
$B^+ \rightarrow K_4^{*+}(2045)\gamma$		90.0	

Table 3: Comparison of upper limits on the branching ratio for the decay $b \rightarrow s\gamma$ ($BR \times 10^3$ at 90% C.L.). The CLEO and ARGUS results are taken from [21] and [22] and are based on the experimental upper limit on the branching ratio for the exclusive mode $B^0 \rightarrow K^{*0}(892)\gamma$ (see Table 2). In the present experiment the result arises from the inclusive measurement of the photon spectrum.

$\frac{\Gamma(B^0 \rightarrow K^{*0}(892)\gamma)}{\Gamma(b \rightarrow s\gamma)}$	$BR(b \rightarrow s\gamma) \times 10^3$		
	CLEO	ARGUS	Crystal Ball
4.5%	6.2	9.3	2.8
40.0%	0.7	1.1	

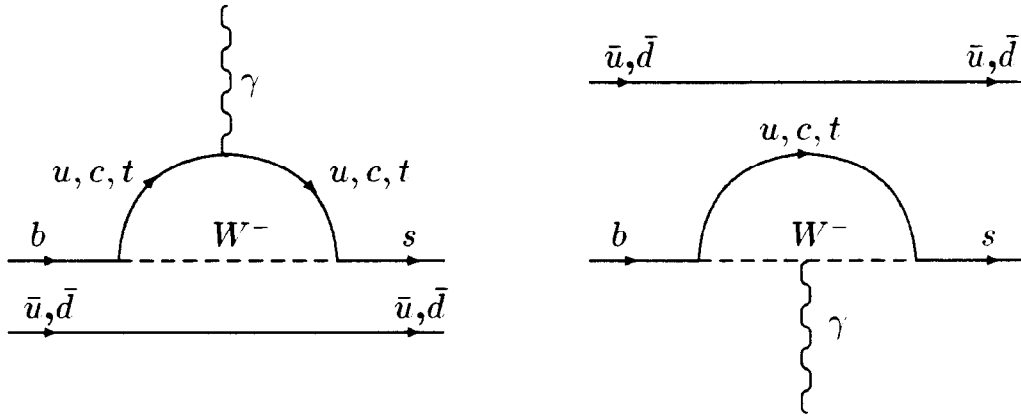


Figure 1: $B \rightarrow K^* \gamma$ penguin diagrams in the Standard Model.

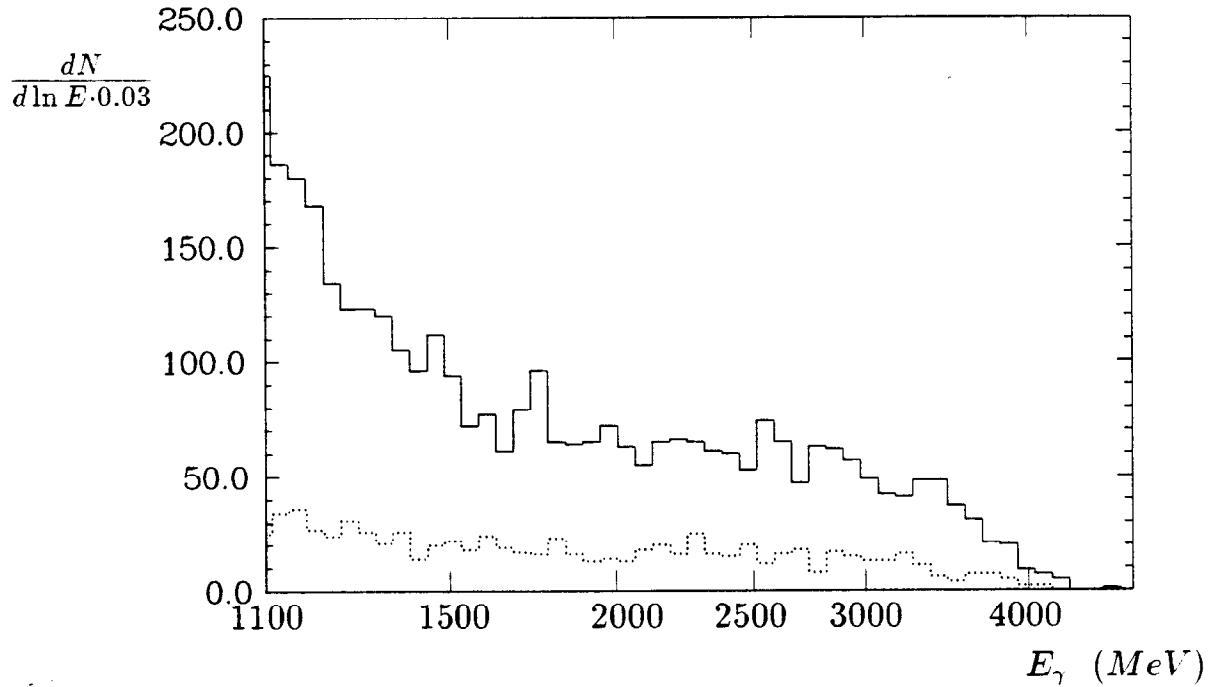


Figure 2: Inclusive spectrum of photons from the ON $\Upsilon(4S)$ (solid histogram) and the continuum (dotted histogram) data samples. We multiply the continuum spectrum by $r = 4.025$ before subtracting it to get Fig. 3.

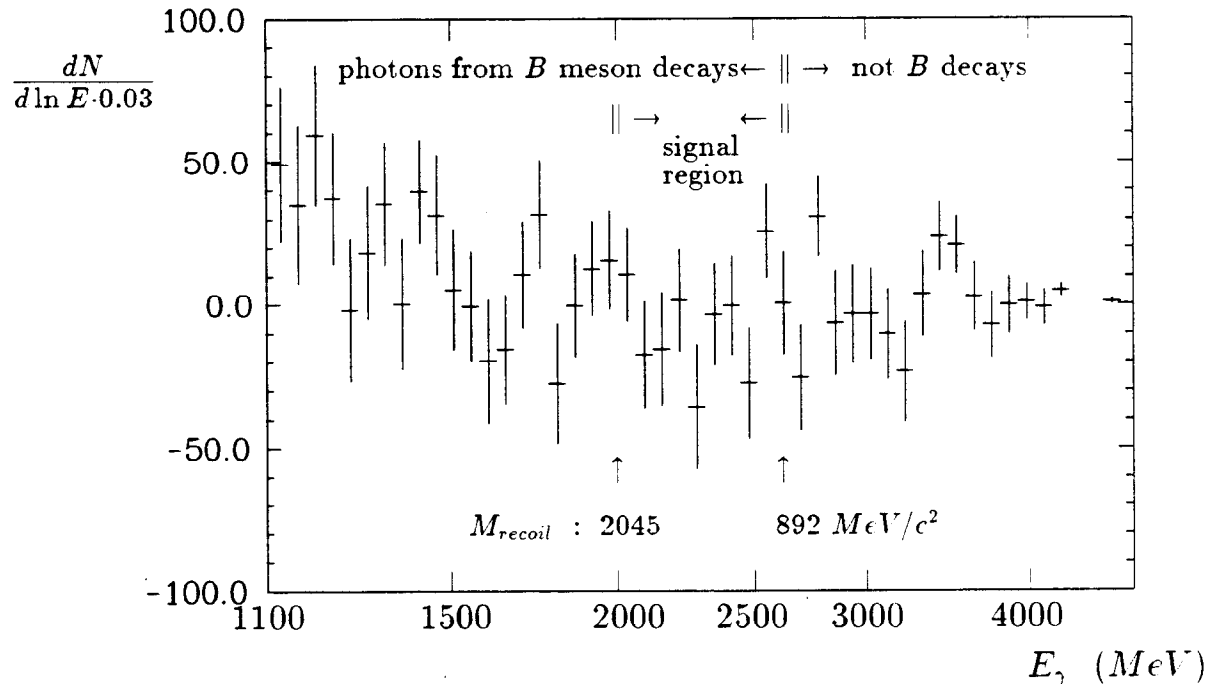


Figure 3: The inclusive photon spectrum from $B\bar{B}$ events (after the subtraction of the continuum contribution from the ON $\Upsilon(4S)$ events).

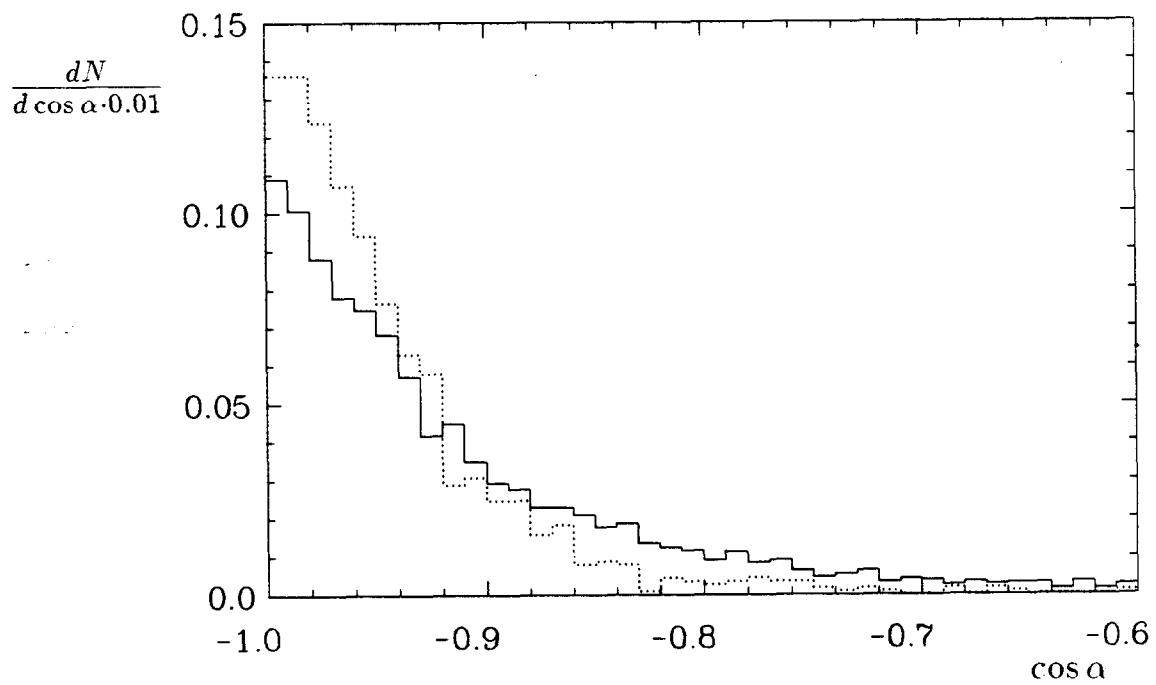


Figure 4: The distributions (normalized to the same area) of the angle between the photon and the 'opposite' particle for ON $\Upsilon(4S)$ data (solid histogram) and a Monte Carlo simulation of the decay chain $\Upsilon(4S) \rightarrow B\bar{B}$, $B \rightarrow K_4^*(2045)\gamma$ (dotted histogram).

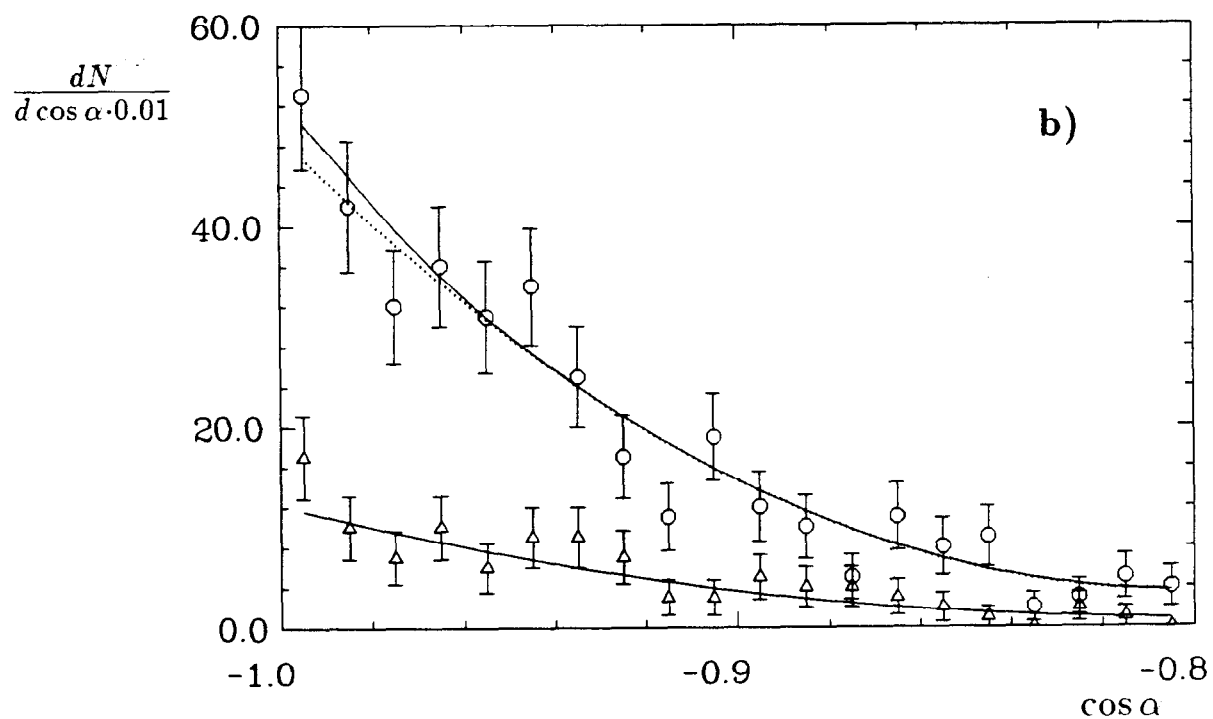
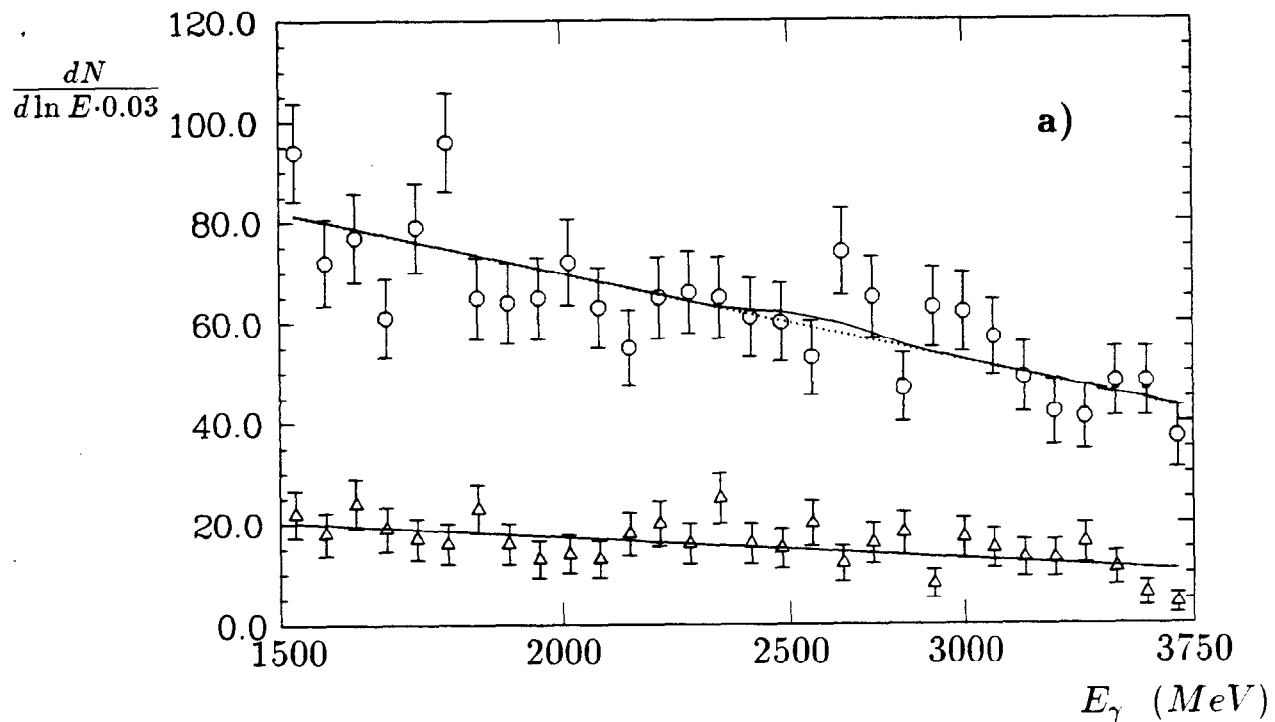


Figure 5: The simultaneous fit (solid line) to (a) the inclusive photon spectrum and (b) to the distribution of the cosine of the angle α between the photon and the 'opposite' particle for ON $\Upsilon(4S)$ (circles) and continuum (triangles) photons in the energy range expected for the $B \rightarrow K^*(892)\gamma$ decay. The area between the solid and dotted line corresponds to the fitted signal.